

Regular and chaotic dynamics of periodically amplified picosecond solitons

Yannis Kominis and Kyriakos Hizanidis

*Department of Electrical and Computer Engineering, National Technical University of Athens,
9 Iroon Polytechniou, 157 73 Athens, Greece*

Received July 25, 2001; revised manuscript received January 2, 2002

Chirped-pulse propagation under periodic amplification is considered on the basis of the variational method, and the resulting pulse-shape chaotic oscillations are studied. The system of equations governing the evolution of the parameter functions is nonintegrable and is solved by the canonical perturbation method and the construction of local approximate invariants embracing all the essential features of the phase-space dynamics. The latter provide useful guidelines for choosing the appropriate launching-pulse width and chirp for stable propagation for each specific transmission-link configuration. This fact is supported by comparison of the analytic results with the respective numerical ones of the exact dynamical system obtained by the variational method and by the direct integration of the nonlinear Schrödinger equation as well. The structure of the chaotic layer between the two distinct modes of behavior of a propagating pulse, namely, breathing and spreading/decaying, is also investigated qualitatively by utilizing Melnikov's method. Examples from technologically realistic configurations are given for 4–14-ps pulses and for amplification periods of 40–100 km.

© 2002 Optical Society of America

OCIS codes: 060.2320, 060.2330, 060.2410, 060.5530, 190.4370, 190.5530.

1. INTRODUCTION

Since an optical soliton has been experimentally demonstrated, its potential use in long-haul, high-speed communications has also been established.¹ Until the discovery of the erbium-doped fiber amplifier, one of the major problems of soliton long-distance propagation was the pulse attenuation due to fiber loss. Reshaping of solitons by means of repeated amplifications with erbium-doped fiber amplifiers was successfully demonstrated more than a decade ago,² and high-bit-rate transmission has been achieved experimentally for propagation distances of the order of thousands of kilometers. The presence of a chain of erbium-doped fiber amplifiers along the transmission line causes a periodic variation of gain that appears as an inhomogeneity in the transmission medium. Another source of inhomogeneity of the propagation medium is the periodic variation of the dispersion, known as dispersion management, which incorporates two or more fiber segments with different group-velocity dispersions and has been proposed as a technique for improving the performance of optical communication systems. Such systems have many beneficial features in comparison with systems with constant group-velocity dispersion, even if the path averages are equal. High local dispersion, for example, significantly reduces the efficiency of four-wave mixing and decreases both the modulational instability and gain. Finally, a periodically modulated core diameter acts like an inhomogeneous propagation medium.³

Pulse propagation under periodic amplification and/or dispersion management has been studied for various cases^{4–11} with the nonlinear Schrödinger equation (NLS), with propagation distance-dependent coefficients being the most often used mathematical model in the scientific

literature, although there are well known limitations that should be carefully taken into account in each particular application. The guiding-center soliton theory has been used in the literature to describe soliton propagation in the case of short-period inhomogeneity, compared with the soliton period (or with dispersion length).¹ The case of weak nonlinearity has also been considered,¹² and a direct perturbation technique based on linearization of the NLS equation has been used to study the effect of periodic amplification.¹³ However, the demand for higher capacity of the transmission systems requires shorter pulses, which means shorter dispersion lengths. Since the inhomogeneity period equals the distance between the amplifiers, which is of the order of a few tens of kilometers, it becomes comparable to or even larger than the dispersion length, and the guiding-center theory cannot be applied. In this case, optical pulses and bit patterns (trains of pulses) experience significant deterioration. This problem can be handled by several techniques that have been proposed in the scientific literature^{14–17}: prechirping, use of higher power for the pulses at the launching optical node, and reshaping passive devices, to mention only a few. Prechirping techniques and the use of high-power optical pulses, however, lead to complex pulse dynamics during propagation.¹⁷ A variational approach^{18,19} can give qualitative and quantitative results for propagation of short pulses in inhomogeneous media. According to the variational method,^{20,21} the evolution of certain parameters of the pulse such as its amplitude, duration, and chirp can be obtained assuming a specific profile for the pulse. However, the variational method is incapable of capturing drastic changes in pulse shape, such as pulse splitting and radiation emission. As far as the latter is concerned, and exclusively for propagation in a homoge-

neous medium, there have been efforts in the framework of the inverse scattering transform.²² Nevertheless, the advantage of the variational method is its capability for providing a clear qualitative picture and good quantitative results when one compares with direct, though time consuming, numerical simulations in inhomogeneous cases^{18,23} (such as the amplification-induced inhomogeneity), where other more accurate methods, when applied in homogeneous cases, fail to predict the dynamics of the evolving pulse shape.

We study the propagation of a chirped soliton in terms of the variational approach. A set of ordinary differential equations for the pulse amplitude, duration, and chirp is obtained as in Refs. 19 and 24. The dynamics of this system is equivalent to the motion of an effective particle under a periodically perturbed Kepler potential. The latter system has a long history; it has been proposed since 1884 by the Swedish astronomer J. A. H. Gylden to describe the secular acceleration of the moon's longitude.²⁵ This system is nonautonomous and nonintegrable, exhibiting all the features of chaotic dynamics. In this paper the canonical perturbation method^{26,27} is used to construct analytically local approximate invariants of the system, according to the famous Kolmogorov–Arnold–Moser (KAM) theorem, treating the inhomogeneity as a perturbation. These invariants contain all the essential features of the phase-space structure of the perturbed system, in the same way as the Hamiltonian or any other functionally dependent quantity (as the action) contains all the information for the phase-space structure of an integrable system. The KAM curves do not exist when the perturbation strength exceeds a threshold value and dynamic stochastic instability occurs. The increasing of the perturbation strength causes what is widely known as resonance overlap,²⁸ which gives rise to chaotic dynamics. However, not all the resonances overlap for the same perturbation strength, and the stochasticization of the motion is not uniform in phase space. An accurate view of the stochasticization of the phase space can be obtained by the Poincaré surfaces of section. The behavior of the constructed approximate invariants, under increasing perturbation, is also investigated. Finally, Melnikov's method^{29–31} is used to construct a Poincaré mapping, valid in the vicinity of the separatrix (parabolic motion) in order to study the structure and the width of the stochastic layer separating bounded motion, corresponding to soliton oscillation, from the unbounded one, which corresponds to soliton spreading and decay. To our knowledge, both the construction of local approximate invariants and the calculation of the stochastic layer on the basis of Melnikov's method are novel in the scientific literature. Few attempts in the past are more or less incomplete,¹⁹ especially since they are confined in a limited region of the corresponding phase space,²⁴ and thorough investigation of the meaning and range of values of the perturbation strength are missing. In this paper, the latter is directly associated with all the relevant parameters involved, for the technical problem in hand, namely, the chirped-pulse propagation under periodic amplification.

The rest of the paper is organized as follows: In Section 2 the model equations are obtained with a standard

variational method. The integrable system that forms the basis for the application of the canonical perturbation method is considered in Section 3, and the dynamics of the perturbed system are investigated in detail in Section 4, where the analytical expressions for the approximate local invariants are given. In Section 5, Melnikov's method is used in order to investigate the chaotic dynamics occurring near the separatrix. Finally, a discussion about the applicability of the methods used in this paper, in realistic and technologically sound cases, is presented in Section 6. In this section the analytical results of the proposed methods are tested against numerical integration of the system of ordinary differential equations and direct simulation of the NLS equation. The main conclusions are summarized in Section 7.

2. MODEL EQUATIONS

The presence of erbium-doped fiber amplifiers along the fiber results in a periodical variation of the gain. The soliton propagation is modeled by the nonlinear Schrödinger equation^{1,24}

$$i \frac{\partial q}{\partial Z} + \frac{1}{2} \frac{\partial^2 q}{\partial T^2} + |q|^2 q = i \gamma_0(Z) q. \quad (1)$$

The distance Z is normalized to the dispersion distance

$$Z_0[\text{m}] = 6.07 \times 10^2 \frac{t_s^2[\text{ps}]}{\lambda^2[\mu\text{m}]D[\text{ps/nm}\cdot\text{km}]}, \quad (2)$$

and the time T , measured in a coordinate system traveling with the group velocity, is normalized to the characteristic time

$$T_0 = \frac{t_s}{1.76}, \quad (3)$$

where t_s is the soliton pulse width, D is the group-dispersion parameter, and λ is the carrier wavelength of the pulse. On the other hand, $\gamma_0(Z)$ is the loss–gain function,

$$\gamma_0(Z) = -\Gamma_0 + \Gamma_1 \sum_{n=-\infty}^{+\infty} \delta(Z - Z_a n), \quad (4)$$

where Z_a is the distance between the amplifiers and Γ_0 is the normalized damping rate, which, for a fiber with a power loss rate of $\delta[\text{dB/km}]$, is given by

$$\Gamma_0 = 7 \times 10^{-2} \frac{t_s^2[\text{ps}] \delta[\text{dB/km}]}{\lambda^2[\mu\text{m}]D[\text{ps/nm}\cdot\text{km}]}. \quad (5)$$

Requiring the mean rate (averaged over a long distance) of the soliton attenuation and amplification to be zero, we have $\Gamma_1 = \Gamma_0/Z_a$. Transforming the complex amplitude q to a new variable u through

$$u(T, Z) = \exp[-\Gamma(Z)]_q(T, Z), \quad (6)$$

where

$$\Gamma(Z) = \int \gamma_0(Z) dZ, \quad (7)$$

we obtain the following equation for u :

$$i \frac{\partial u}{\partial Z} + \frac{1}{2} \frac{\partial^2 u}{\partial T^2} + \exp[2\Gamma(Z)]|u|^2 u = 0. \quad (8)$$

The variational approach is then applied. The following trial function, representing a chirped soliton, is selected:

$$u(Z, T) = A(Z) \operatorname{sech} \left[\frac{T}{\alpha(Z)} \right] \exp[i\phi_0(Z)T^2], \quad (9)$$

where $A(Z)$, $\alpha(Z)$, and $\phi_0(Z)$ are the amplitude, duration, and frequency chirp of the soliton pulse, respectively.

In order to study the evolution of these quantities, under the propagation along Z , we use the Lagrangian of Eq. (8),

$$L = i \left(u \frac{\partial u^*}{\partial Z} - u^* \frac{\partial u}{\partial Z} \right) + \left| \frac{\partial u}{\partial T} \right|^2 - \exp[2\Gamma(Z)]|u|^4 \quad (10)$$

averaged over the time T ,

$$\langle L \rangle = \int_{-\infty}^{\infty} L dT. \quad (11)$$

The equations governing the evolution of the soliton amplitude, duration, and chirp are obtained from the variation equation

$$\delta \int_0^T \langle L \rangle dZ = 0, \quad (12)$$

leading to the following system of equations,

$$\phi_0 = \frac{1}{2} \frac{d(\ln \alpha)}{dZ}, \quad (13)$$

$$\frac{d(\alpha|A|^2)}{dZ} = 0, \quad \alpha|A|^2 = N^2 = \text{const.}, \quad (14)$$

$$\frac{d^2 \alpha}{dZ^2} = \frac{4}{\pi^2 \alpha^3} - \frac{4N^2 \exp[\Delta(Z)]}{\pi^2 \alpha^2}, \quad (15)$$

$$\frac{d(\arg A)}{dZ} = -\frac{1}{3\alpha^2} + \frac{5}{6} \frac{N^2 \exp[\Delta(Z)]}{\alpha}, \quad (16)$$

where the function $\Delta(Z)$ is defined as

$$\Delta(Z) = \frac{4}{\pi} \Gamma(Z) \quad (17)$$

and can be decomposed into the Fourier series²⁴

$$\Delta(Z) = \frac{4}{\pi^2} \Gamma_1 \sum_{n \neq 0} \frac{n^{-1}}{2i} \exp \left(i \frac{2\pi n}{Z_a} Z \right). \quad (18)$$

The evolution of the soliton duration α is equivalent to the motion of a particle with a unit mass under the influence of a perturbed Kepler potential, where Z is the time, as can be seen in Eq. (15).

Before proceeding to the time-periodic perturbed Kepler problem, some of the characteristics of the unperturbed Kepler problem are discussed. This provides the necessary basis for the perturbation method, which is employed next.

3. UNPERTURBED KEPLER PROBLEM

The potential energy for the unperturbed Kepler problem is

$$U = \frac{2}{\pi^2 \alpha^2} - \frac{4N^2}{\pi^2 \alpha}, \quad (19)$$

and it has a minimum at $\alpha_{\min} = 1/N^2$, where it is equal to $U_{\min} = -2N^4/\pi^2$. The oscillatory or unbounded character of the motion depends on the initial value of the total energy of the associated particle

$$E_0 = \frac{2}{\pi^2 \alpha_0^2} - \frac{4N^2}{\pi^2 \alpha_0} + 2\alpha_0^2 \phi_0^2. \quad (20)$$

For $E_0 < 0$ the motion is oscillatory, and for $E_0 > 0$ the motion is unbounded. The separatrix motion for initial energy $E_0 = 0$ corresponds to an unbounded parabolic orbit. We remark that, under the perturbation, a stochastic layer is generated between the two kinds of motion, the width of which is the subject of a subsequent section.

The Hamiltonian (and the total energy) of the particle is

$$H_0 \left(\alpha, \frac{d\alpha}{dZ} \right) = \frac{1}{2} \left(\frac{d\alpha}{dZ} \right)^2 + \frac{2}{\pi^2 \alpha^2} - \frac{4N^2}{\pi^2 \alpha} = E. \quad (21)$$

Since the evolution of α is oscillatory for $E_0 < 0$, it can be represented by a Fourier series

$$\alpha(Z) = \sum_m \alpha_m \exp(-im\omega Z), \quad \alpha_m = \frac{2b}{m} J'_m(e_0 m), \quad (22)$$

where the prime denotes a differentiation of a Bessel function with respect to its argument. The Fourier components are given in terms of the set of parameters of the orbit commonly used in celestial mechanics,

$$\alpha(Z) = b[1 - e_0 \cos(\xi)], \quad \omega Z = \xi - e_0 \sin(\xi), \quad (23)$$

$$e_0 = \sqrt{1 - \frac{\pi^2 |E|}{2N^4}}, \quad b = \frac{2N^2}{\pi^2 |E|}. \quad (24)$$

The Fourier series of the function $1/\alpha(Z)$, also necessary for the analysis that follows, is given by

$$\frac{1}{\alpha(Z)} = \sum_m c_m \exp(-im\omega Z), \quad c_m = \frac{2}{b} J_m(e_0 m). \quad (25)$$

For the oscillatory kind of motion, the unperturbed problem is transformed to the action-angle variables, as a first step in applying the canonical perturbation method. The action-angle variables are defined as

$$J = \frac{1}{2\pi} \oint \left(\frac{d\alpha}{dZ} \right) dZ = \frac{2\sqrt{2}N^2}{\pi^2 \sqrt{-E}} - \frac{2}{\pi}, \quad (26)$$

$$\theta = \xi - e_0 \sin \xi. \quad (27)$$

The Hamiltonian of the transformed problem is given by

$$H_0(J) = -\frac{8N^4}{\pi^2} \frac{1}{(\pi J + 2)^2} = E, \quad (28)$$

and the frequency of the oscillations is

$$\omega(J) = \frac{dH_0}{dJ} = \frac{16N^4}{\pi} \frac{1}{(\pi J + 2)^3}. \quad (29)$$

The frequency has a maximum value of $\omega_0 = 2N^4/\pi$ for small (linear) oscillations at the bottom of the potential well, where $J = 0$, and goes to zero as it approaches the separatrix, where J goes to infinity.

The harmonic content of the linear spectrum of the unperturbed oscillations along with the spectrum of the perturbing function defines, as is seen below, all the important features of the perturbed-system dynamics. A measure of the spectrum width of the oscillations is the number of the harmonics,

$$N_0 = \frac{1}{8}(\pi J + 2)^3, \quad (30)$$

which ranges between unity, for small (linear) oscillations near the minimum of the potential, and infinity for the aperiodic motion near the separatrix.

4. RESONANT AND CHAOTIC OSCILLATIONS OF THE SOLITON DURATION AND AMPLITUDE

The Hamiltonian of the unperturbed system contains the complete structure of the phase space of the problem. The system is integrable with the time-independent Hamiltonian being an invariant of the motion. The action J is also a constant of the motion functionally dependent on the Hamiltonian. The phase space of the unperturbed system in terms of the transformed action-angle variables (J, θ) is simply obtained as the one-parameter family of level curves, $H_0 = \text{const}$, of the Hamiltonian. Since the Hamiltonian is a function of the action only, this family coincides with the family of concentric circles with radius $J = \text{const}$, $J \in [0, \infty)$, and $\theta \in [0, 2\pi]$. However, the perturbed system is nonautonomous and nonintegrable since there is no second invariant of the motion. The perturbed Hamiltonian,

$$H(J, \theta, Z) = H_0(J) + \epsilon H_1(J, \theta, Z), \quad (31)$$

$$H_1(J, \theta, Z) = -\frac{4N^2}{\pi^2} \frac{1}{\alpha(J, \theta)} \Delta(Z), \quad (32)$$

is no longer a function of the action only. The phase space is four dimensional, and the (J, θ) plane considered as a projection of the phase space or as a Poincaré surface of section does not consist of concentric circles since there is no more cylindrical symmetry (θ independence). According to the KAM theorem, for small perturbations of an integrable system the invariants of the motion persist, although modified, sufficiently far from an exact resonance between the two degrees of freedom. These approximate invariants can be calculated with use of the canonical perturbation theory^{26,27}. One seeks a transformation to new variables $(\bar{J}, \bar{\theta})$ for which the new

Hamiltonian \bar{H} is solely a function of the new action. This procedure can be carried at any desired order in ϵ (which is a bookkeeping parameter for tracking the order of approximation). Since the system is near-integrable, a near-identity canonical transformation of the form

$$S = \bar{J}\theta + \epsilon S(\bar{J}, \theta, Z) \quad (33)$$

is used. This transformation renders the old variables in terms of the new and results in a new Hamiltonian,

$$\bar{H} = H(J, \theta, Z) + \epsilon \frac{\partial S_1(\bar{J}, \theta, Z)}{\partial Z}. \quad (34)$$

Expanding in ϵ , at zero and first order,

$$\bar{H}_0 = H_0(\bar{J}), \quad (35)$$

$$\bar{H}_1 = \frac{\partial S_1}{\partial Z} + \omega \frac{\partial S_1}{\partial \theta} + H_1. \quad (36)$$

Choosing S_1 to eliminate the oscillating part of H_1 , denoted by $\{H_1\}$, we have

$$\bar{H} = H_0 + \epsilon \langle H_1 \rangle, \quad (37)$$

where $\langle H_1 \rangle$ represents the average, over both the θ and Z oscillations, part of H_1 , and

$$\frac{\partial S_1}{\partial Z} + \omega \frac{\partial S_1}{\partial \theta} = -\{H_1\}. \quad (38)$$

Substituting the Fourier expansions (18) and (25) in Eq. (32), one obtains the average and the oscillatory part of the perturbation,

$$\langle H_1 \rangle = 0, \quad (39)$$

$$\{H_1\} = \frac{16N^2}{\pi^4} \frac{\Gamma_1}{b} \sum_{\substack{m \\ n \neq 0}} in^{-1} J_m(e_0 m) \exp(in\Omega Z - im\theta), \quad (40)$$

with $\Omega = 2\pi/Z_a$. The new Hamiltonian to first order in ϵ [Eq. (37)] is identical to the old one, resulting in a zero change in frequency due to perturbation,

$$\Delta\omega = \frac{\partial \langle H_1 \rangle}{\partial J} = 0. \quad (41)$$

Then, S_1 can be obtained from Eq. (38):

$$S_1 = -\frac{16N^2}{\pi^4} \frac{\Gamma_1}{b} \sum_{\substack{m \\ n \neq 0}} \frac{n^{-1} J_m(e_0 m)}{n\Omega - m\omega(J)} \exp(in\Omega Z - im\theta). \quad (42)$$

Finally, the new action, as given by the canonical transformation equations, is

$$\begin{aligned} \bar{J} &= J - \epsilon \frac{16N^2}{\pi^4} \frac{\Gamma_1}{b} \sum_{m, n \neq 0} \frac{imn^{-1} J_m(e_0 m)}{n\Omega - m\omega(J)} \\ &\quad \times \exp(in\Omega Z - im\theta) \\ &= \text{const}. \end{aligned} \quad (43)$$

\bar{J} is an approximate, to first order, invariant of the motion. Setting $\epsilon = 1$, we can obtain the (J, θ) plane of the phase space as the one-parameter family of \bar{J} -level curves.

The new action is no longer θ independent, and the cylindrical symmetry is destroyed. The distortion of the perturbed action in comparison with the unperturbed one is proportional to the strength of perturbation but is not uniform in the (J, θ) plane. When J is near a resonant value J_{mn} , i.e., given by

$$m\omega(J_{mn}) - n\Omega = 0 \tag{44}$$

for a specified pair (m, n) , the distortion is more significant because of the presence of a small denominator in the ϵ -order term in Eq. (43), which increases to infinity, resulting in a drastic change in the topology of the invariant curves and failure of the canonical perturbation theory. Fortunately, there is a simple method to overcome the problem of the small denominators, namely, the global removal of resonances.^{26,32} Since for the unperturbed system ($\epsilon = 0$) the J - θ invariant curves are straight lines ($J = \text{const.}$), an arbitrary function $I_0(J)$

also generates these lines [$I_0(J) = \text{const.}$]. Using $I_0(J)$ instead of J , after some elementary analysis, the canonical perturbation theory results in

$$\begin{aligned} I &= I_0(J) - \epsilon \frac{dI_0}{dJ} \frac{16N^2 \Gamma_1}{\pi^4} \frac{1}{b} \\ &\times \sum_{m,n \neq 0} \frac{imn^{-1}J_m(e_0m)}{n\Omega - m\omega(J)} \exp(in\Omega Z - im\theta) \\ &= \text{const.} \end{aligned} \tag{45}$$

$I_0(J)$ can be chosen so that dI_0/dJ vanishes at the resonant values J_{mn} to ensure that the ϵ -order term in Eq. (45) remains actually small even at resonances. Even though it is difficult to choose $I_0(J)$ so that all resonant denominators are removed, there are simple and suitable choices of $I_0(J)$ that can be used in order to “remove” entire sets of resonances. Indeed, if we set

$$\frac{dI_0}{dJ} = \sin\left[\frac{\pi\Omega}{\omega(J)}\right], \tag{46}$$

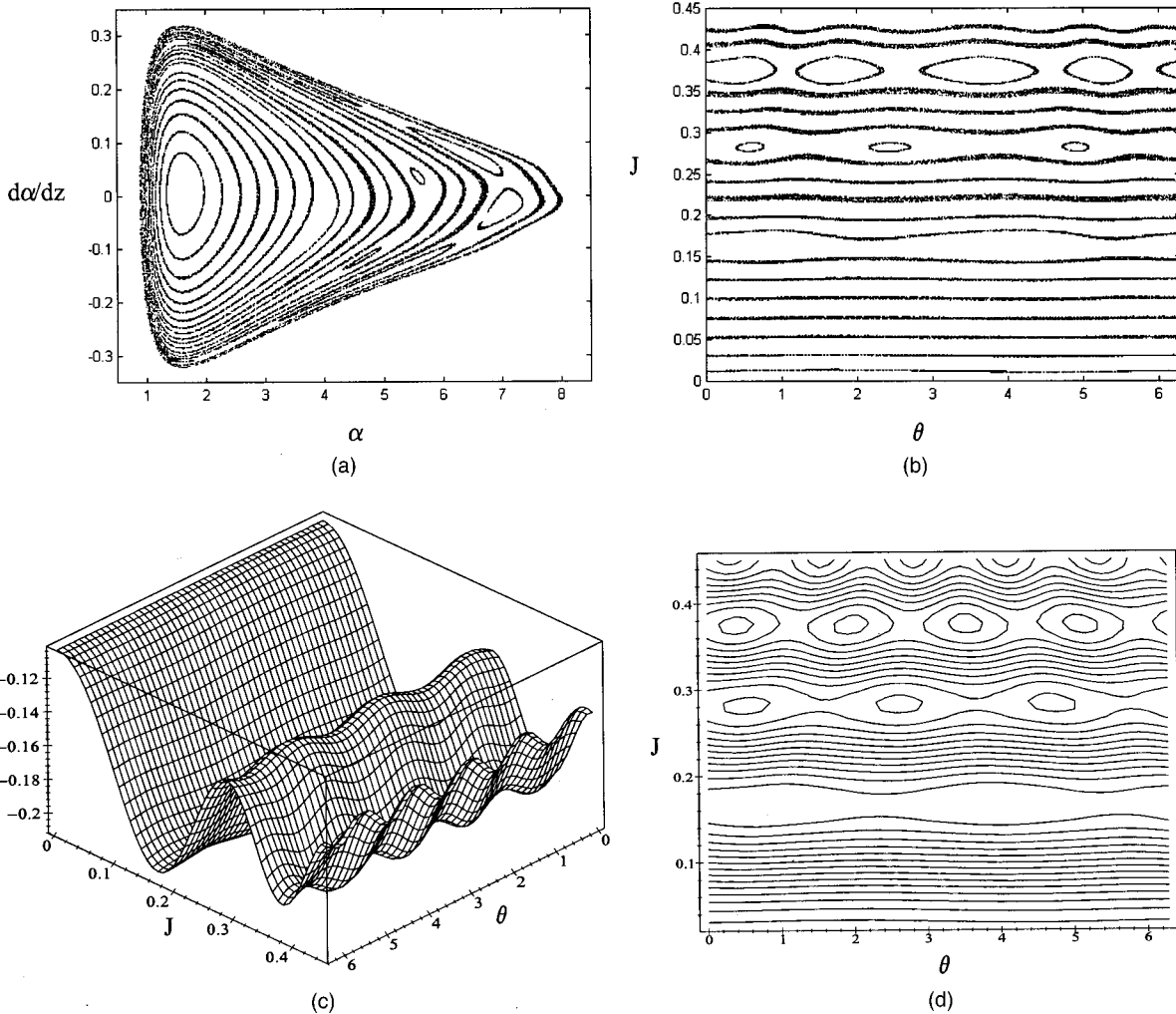


Fig. 1. Propagation of a soliton of duration $t_s = 4$ ps under amplification period $d = 100$ km. $N = 0.793$, corresponding to $\omega_0 = \Omega$: (a) phase-plane diagram in terms of the original variables, (b) phase-plane diagram in terms of action-angle, (c) analytically constructed approximate invariant, and (d) the corresponding contour plot.

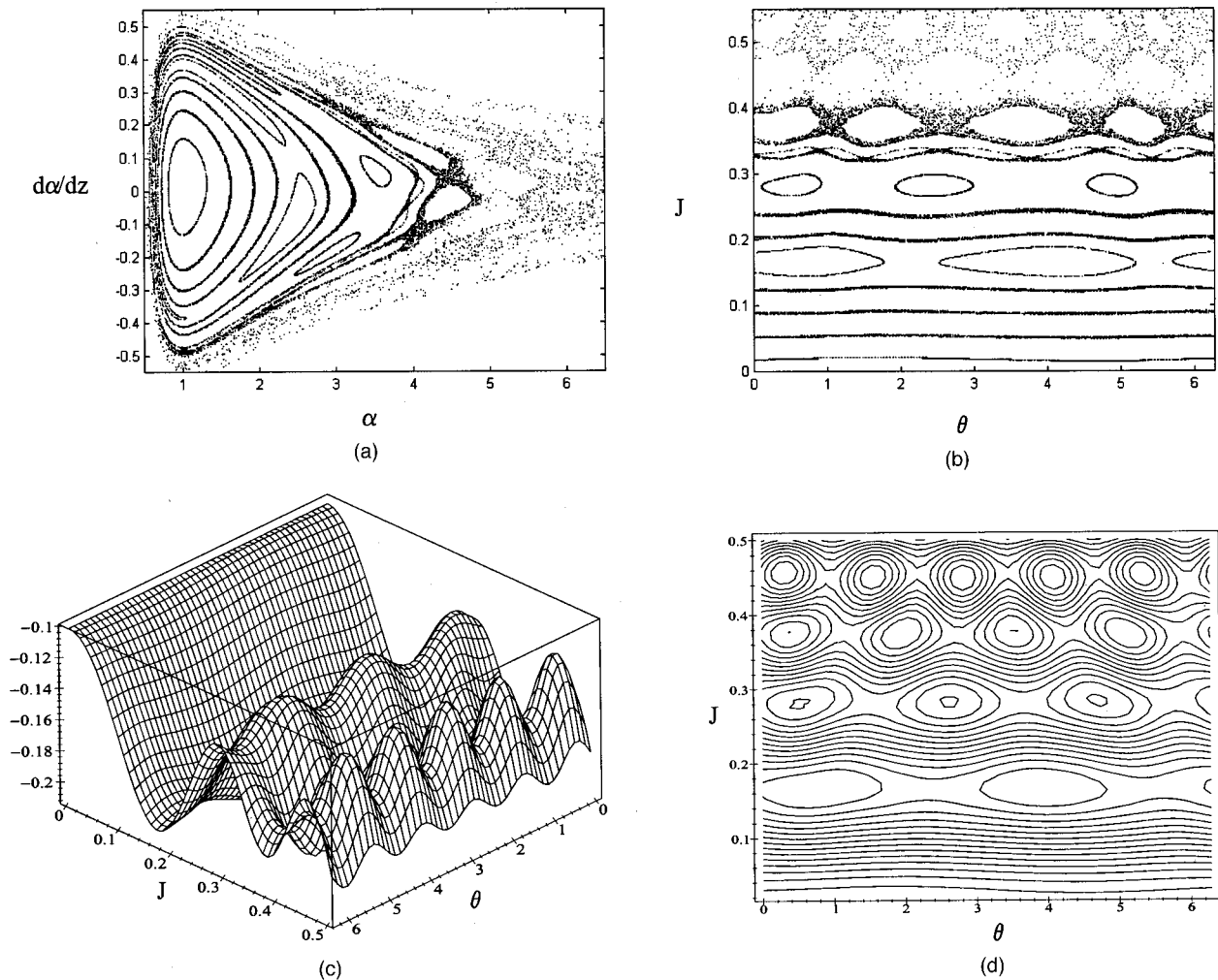


Fig. 2. Propagation of a soliton of duration $t_s = 4$ ps under amplification period $d = 40$ km. $N = 0.997$, corresponding to $\omega_0 = \Omega$: (a) phase-plane diagram in terms of the original variables, (b) phase-plane diagram in terms of action-angle, (c) analytically constructed approximate invariant, and (d) the corresponding contour plot.

the $(m, n = 1)$ set of resonances can be removed. The one-parameter family of the level curves of Eq. (45) give with satisfying accuracy the (J, θ) phase plane if one neglects all but the first harmonics of Ω .

For the resonant action values, as we have seen, there is a drastic change in the topology of the perturbed-system phase space, appearing as a ring of m “islands.” The width of these islands (i.e., the resonance width²⁶) is

$$\Delta J_{mn} = 2 \left| \frac{2 \frac{16N^2 \Gamma_1}{\pi^4} \frac{1}{b} n^{-1} J_m(e_0 m)}{\frac{d\omega}{dJ}} \right|_{J=J_{mn}}^{1/2} \quad (47)$$

The resonance width increases with perturbation, and stochastic instability develops when two neighboring islands overlap, giving rise to chaotic dynamics.²⁸ The overlap condition is given in terms of the parameter s ,

$$s = \frac{1}{2} \frac{\Delta J_{mn} + \Delta J_{m'n'}}{\delta J_{mn}}, \quad (48)$$

where $(m, n), (m', n')$ are neighboring resonances and $\delta J_{mn} = |J_{mn} - J_{m'n'}|$ is the distance between action resonant values. Most of the invariant KAM curves between two resonances are destroyed for $s \geq 1$, and the actual structure of the phase space for the transitional region $0.7 \leq s \leq 1.5$ can be quite complicated.

In order to complete the picture of the phase space and the (J, θ) plane, one should realize that a KAM invariant curve can be close to a resonance as a rational number can be close to an irrational number, and two resonances can also be as close as two rational ones. However, the width of each resonance depends on the Fourier components of the unperturbed solution c_m and the periodic perturbation ($\sim n^{-1}$), which decreases for increasing m and n ; thus resonances corresponding to larger m and n are less significant. This means that although very close to the $(1, 2)$ resonance, there exist the $(11, 20)$, $(21, 40)$, and infinitely many other resonances, the latter of which are

negligible. Also, after choosing an amplifier spacing Z_a (and Ω), not all the resonances (m, n) exist (at least to first order in ϵ), since $\omega \leq 2N^4/\pi$ so that the resonance condition (44) does not have a solution for J for every (m, n) .

5. WIDTH OF THE STOCHASTIC LAYER SEPARATING OSCILLATORY AND DECAYED SOLITONS

In the unperturbed Kepler problem, oscillatory motion, corresponding to soliton existence, is separated from the unbounded motion, corresponding to soliton decay, by the parabolic orbit $E = 0$. Under sufficiently strong perturbation, there exists the possibility of chaotic transition from the oscillatory kind of motion to the unbound one. This could happen for certain initial conditions that are far enough from the resonant centers and/or near the (unperturbed) separatrix ($E = 0$). There the motion is of intermittent character, so that the effective particle may be captured for a few periods close to a resonant center before it escapes to infinity. A stochastic layer is formed close to the (unperturbed) separatrix; thus if the initial

energy E_0 falls into this layer, the soliton can stochastically escape from the potential well and decay. The dynamics inside the layer are equivalent to the well known “horseshoe” map chaotic dynamics.²⁹ In order to establish a condition under which chaotic dynamics occur near the separatrix and an estimation of the width of this chaotic region, Melnikov’s method can be used. The Melnikov’s function $M(Z_0)$ is related to the distance between the stable and unstable manifold of the hyperbolic fixed point $(\alpha, \alpha_z) = (0, 0)$ on a Poincaré surface of section Σ^{Z_0} and is defined as

$$M(Z_0) = \int_{-\infty}^{+\infty} [H_0, H_1][\alpha_0(Z)]dZ, \tag{49}$$

where $[H_0, H_1]$ denotes the Poisson bracket

$$[H_0, H_1] = \frac{\partial H_0}{\partial \alpha} \frac{\partial H_1}{\partial \alpha_z} - \frac{\partial H_0}{\partial \alpha_z} \frac{\partial H_1}{\partial \alpha}, \tag{50}$$

and $\alpha_0(Z)$ is the unperturbed parabolic orbit.

Substituting Eqs. (21) and (32) and integrating by parts yields

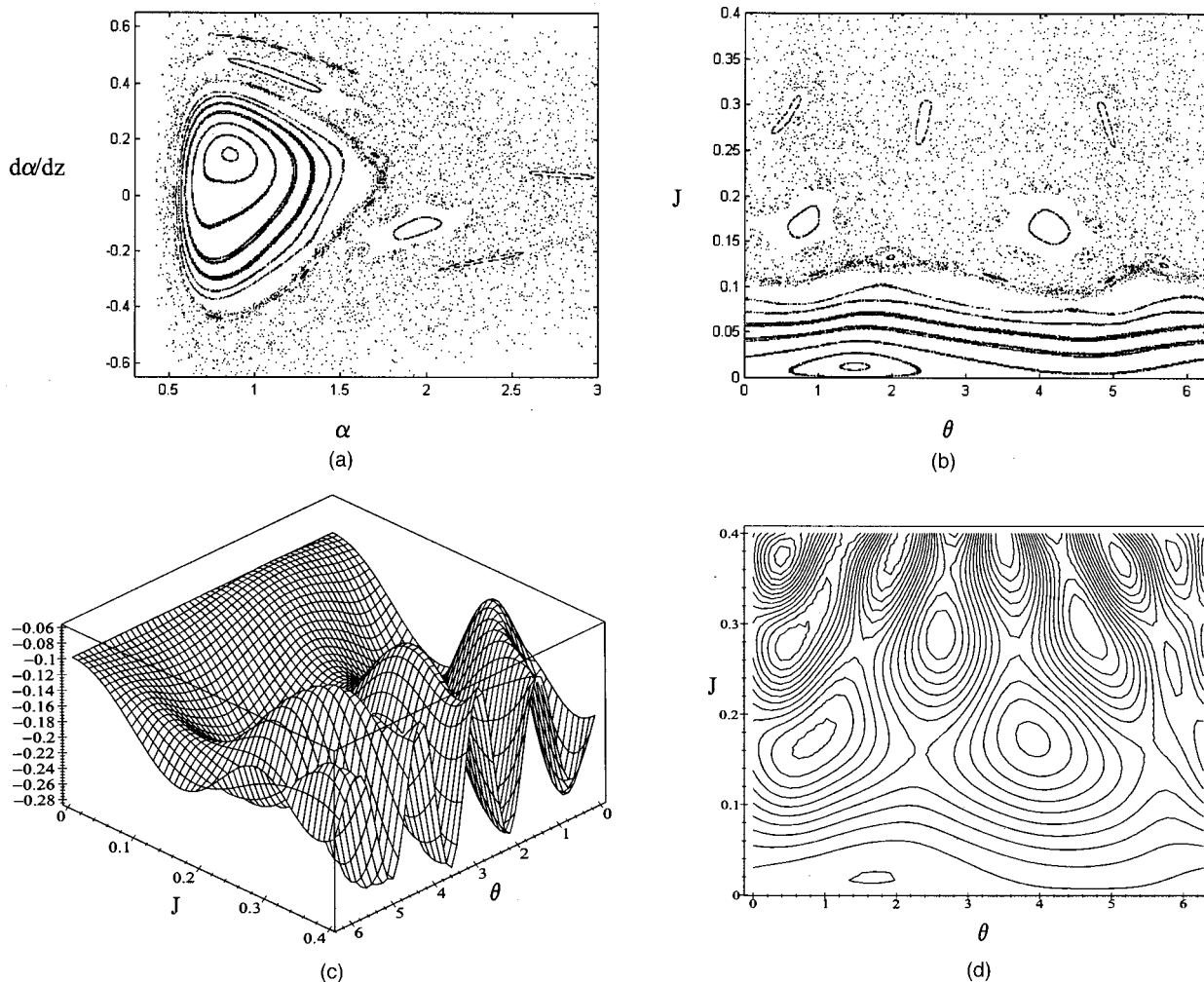


Fig. 3. Propagation of a soliton of $t_s = 8$ ps duration under amplification period $d = 100$ km. $N = 1.121$, corresponding to $\omega_0 = \Omega$: (a) phase-plane diagram in terms of the original variables, (b) phase-plane diagram in terms of action–angle, (c) analytically constructed approximate invariant, and (d) the corresponding contour plot.

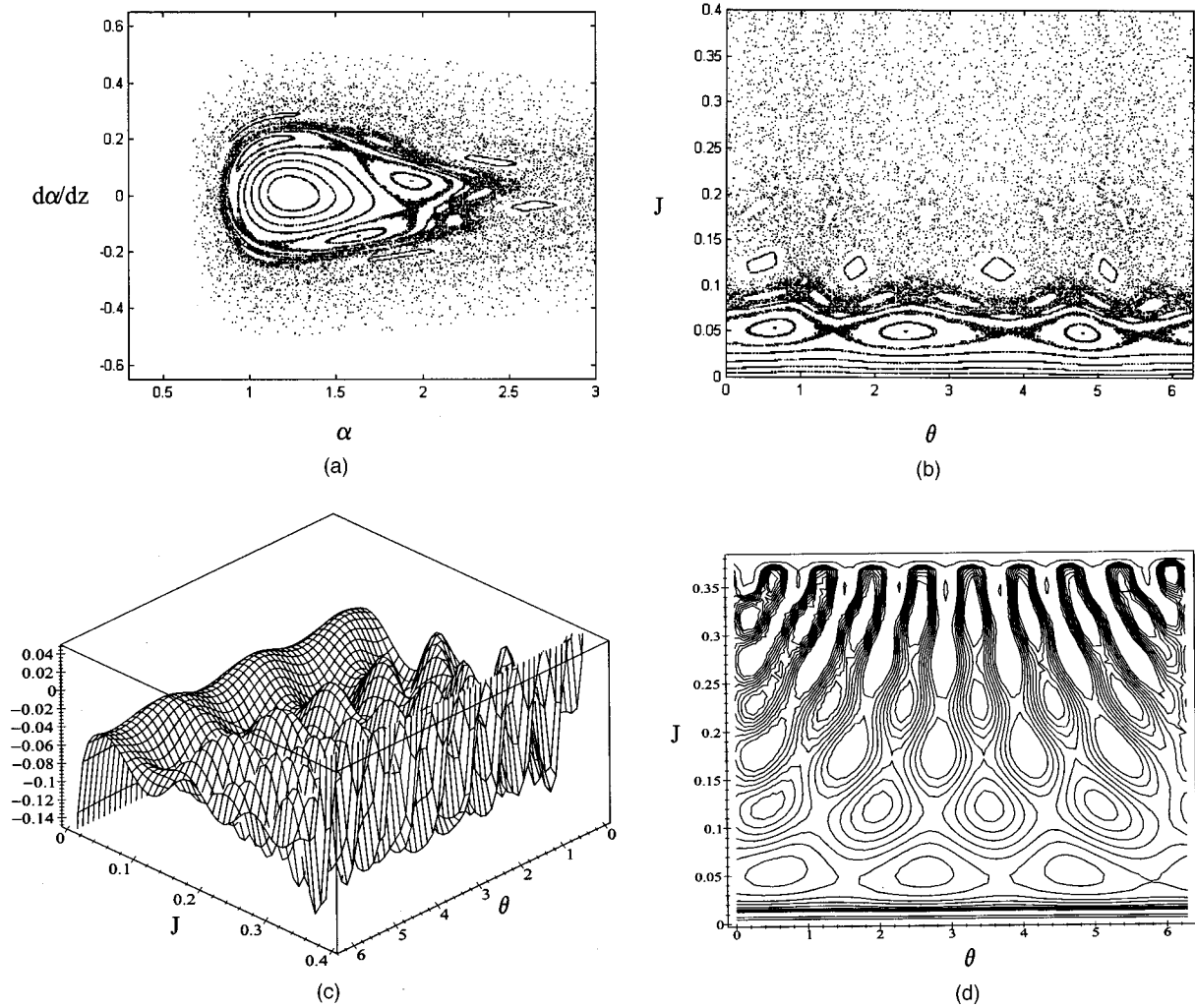


Fig. 4. Propagation of a soliton of $t_s = 8$ ps duration under amplification period $d = 100$ km. $N = 0.9$, corresponding to $\omega_0 \leq \Omega$: (a) phase-plane diagram in terms of the original variables, (b) phase-plane diagram in terms of action-angle, (c) analytically constructed approximate invariant, and (d) the corresponding contour plot.

$$M(Z_0) = -\frac{4N^2}{\pi^2} \int_{-\infty}^{+\infty} \frac{\alpha_{0z}(Z)}{\alpha_0^2(Z)} \Delta(Z + Z_0) dZ$$

$$= -\frac{16N^2}{\pi^4} \Gamma_1 \sum_{n=1}^{\infty} n^{-1} \cos(n\Omega Z_0) I_n, \quad (51)$$

$$I_n = \int_{-\infty}^{+\infty} \frac{\alpha_{0z}(Z)}{\alpha_0^2(Z)} \sin(n\Omega Z) dZ. \quad (52)$$

Using the expression of $\alpha_0(Z)$ as a function of the true anomaly v , given by

$$\alpha_0(Z) = \frac{1}{1 + \cos v}, \quad (53)$$

and the fact that parabolic motion implies that

$$Z = \frac{k^3}{4} \left[\tan\left(\frac{v}{2}\right) + \frac{1}{3} \tan^3\left(\frac{v}{2}\right) \right], \quad (54)$$

one obtains

$$I_n = \frac{4}{3} \Omega k^3 \sin\left(\frac{\pi}{3}\right) K_{1/3}\left(\frac{n 2N^2 \Omega k^3}{3\pi^2}\right), \quad (55)$$

where $k = \pi^2/4N^4$, and $K_{1/3}$ is the modified Bessel function of the first kind, which tends exponentially to zero when its argument tends to infinity through positive values.³⁰

Since $M(Z_0)$ has simple zeros in the interval $[0, Z_a)$, the stable and unstable manifolds intersect transversely, and the dynamics near the separatrix are equivalent to the dynamics of the “horseshoe” map. Melnikov’s function also gives the energy change ΔE due to the perturbation and can be used to construct the following separatrix mapping:

$$E_{k+1} = E_k + \Delta E\left(\frac{\phi_k}{\Omega}\right),$$

$$\phi_{k+1} = \phi_k + \Omega T(E_{k+1}). \quad (56)$$

The structure and the width of the stochastic layer can be studied by iterating the separatrix mapping over many periods of the perturbing function.

6. DISCUSSION

In the following, the case of a pulse with carrier wavelength $\lambda = 1.55 \mu\text{m}$ propagating in a typical line optical fiber with dispersion $D = 1 \text{ ps}/(\text{nm km})$ and power loss rate $\delta = 0.2 \text{ dB/km}$ is considered. The effective perturbation is $\epsilon = 5.88 \times 10^{-4} t_s^4/d$, where t_s is given in picoseconds, and d is the actual distance between the amplifiers in kilometers ($d = Z_a \times Z_0$). We remark that varying the amplifiers distance, for a constant soliton pulse width t_s , affects both the strength of the perturba-

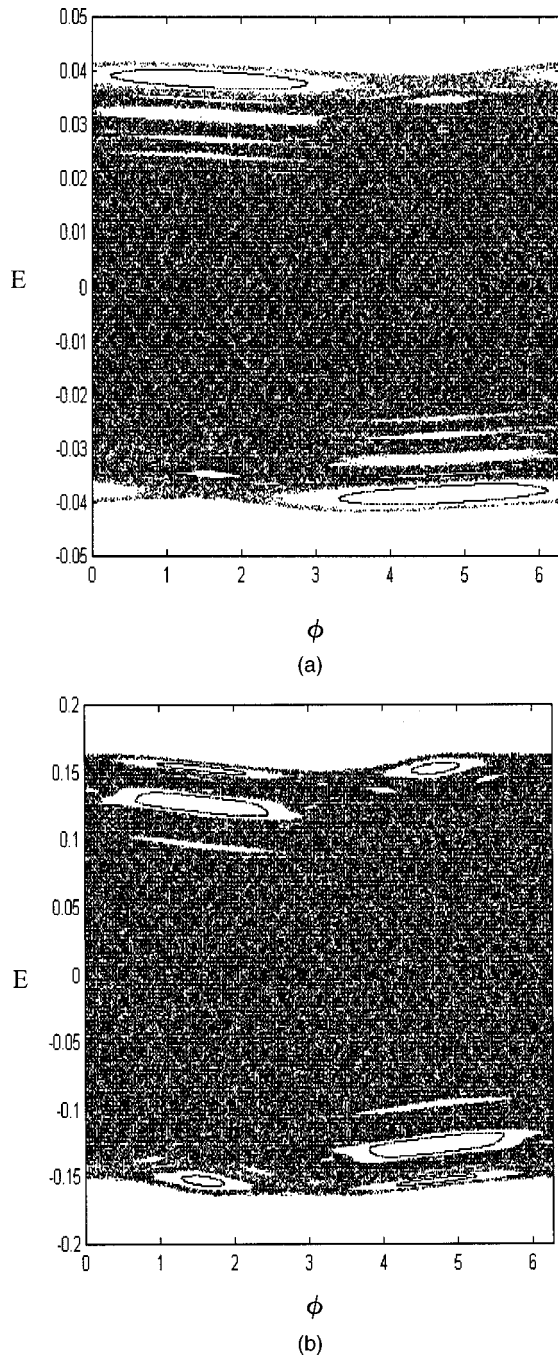


Fig. 5. Iterations of the separatrix map: (a) $t_s = 4 \text{ ps}$ duration under amplification period $d = 100 \text{ km}$, $N = 0.793$, corresponding to $\omega_0 = \Omega$; (b) $t_s = 4 \text{ ps}$ duration under amplification period $d = 40 \text{ km}$, $N = 0.997$, corresponding to $\omega_0 = \Omega$.

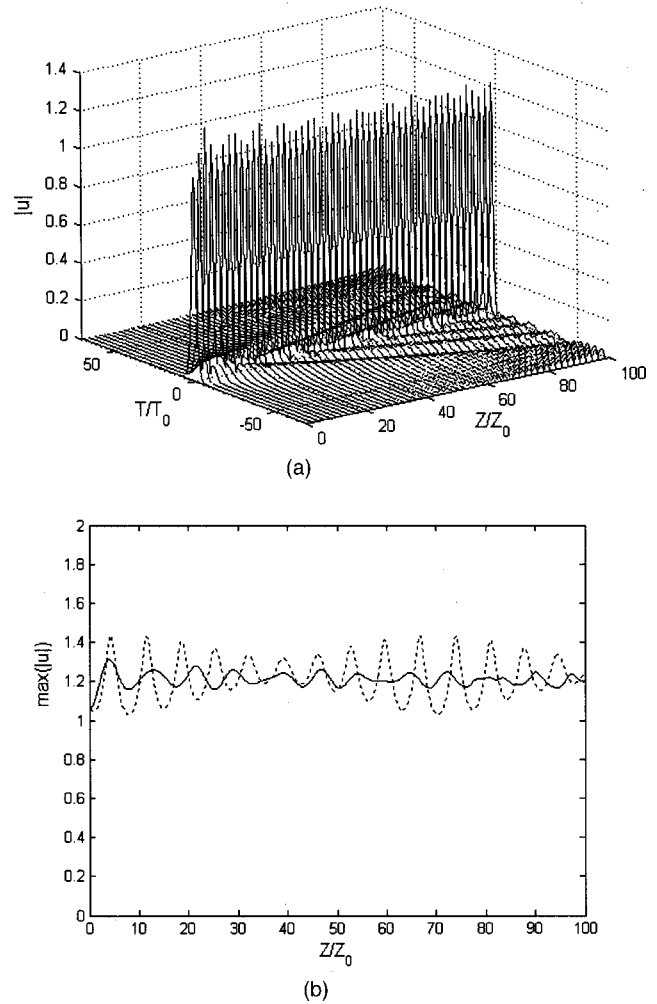


Fig. 6. Nonlinear shape oscillations of a soliton of $t_s = 8 \text{ ps}$ duration under amplification period $d = 100 \text{ km}$. $N = 1.121$, corresponding to $\omega_0 = \Omega$. The initial width and chirp correspond to the point $(\alpha, \alpha') = (1.1, 0.1)$ in Fig. 3(a): (a) numerical integration of the NLS equation; (b) comparison of the direct simulation (solid curve) with the variational method (dashed curve).

tion and the frequency of the perturbing function $\Delta(Z)$, resulting in variations in the resonance width and location. The function $I_0(J)$ is computed in terms of Taylor series. The results obtained by the numerical integration of the dynamical system are compared with those based on the canonical perturbation method in the following four figures of Fig. 1: (a) the phase plane in terms of the original variables (α, α_Z) , (b) the phase plane in terms of action-angle variables (J, θ) , with the analytical results obtained by use of the canonical perturbation theory, (c) the approximate invariant $I(J, \theta)$, and (d) the phase plane in terms of action-angle variables (J, θ) obtained as the one-parameter family of level curves of I .

In Fig. 1 the pulse width is $t_s = 4 \text{ ps}$, and the amplification period $d = 100 \text{ km}$. In such a case the normalized distance between the amplifiers is 25 times larger than the dispersion distance Z_0 ($Z_a = 25$), and the effective perturbation is then $\epsilon = 0.0015$. We have also taken $N = 0.793$ so that $\omega_0 = \Omega$. It is evident that the analytical results in Fig. 1(d) are quite similar to the numerical ones in Fig. 1(b). In Fig. 2 the amplification period is

smaller, namely, $d = 40$ km. The normalized distance between the amplifiers is now 10 times larger than the dispersion distance $Z_0 (Z_a = 10)$, and the effective perturbation is increased to $\epsilon = 0.004$. We also take $N = 0.997$ so that $\omega_0 = \Omega$. The stronger perturbation causes an increased width of the islands of regular behavior and the emerging of a stochastic layer near the separatrices as well. The latter is very significant, especially for the (4, 1) (and higher) resonances, as shown in Fig. 2(b). The analytical results in Fig. 2(d) are still in good agreement with the numerical ones. However, the stochastic layers cannot be captured by the canonical perturbation theory.

In Fig. 3 the pulse width is $t_s = 8$ ps, and the amplification distance is $d = 100$ km. The normalized distance between the amplifiers is 6.25 times larger than the dispersion distance $Z_0 (Z_a = 6.25)$, and the effective perturbation is $\epsilon = 0.024$. We also take $N = 1.121$ so that $\omega_0 = \Omega$. The region between the (2, 1) and the (3, 1) resonances is quite chaotic. The two resonances overlap, and there is no invariant (KAM) curve between them. The overlapping of the two resonances is exhibited in Fig.

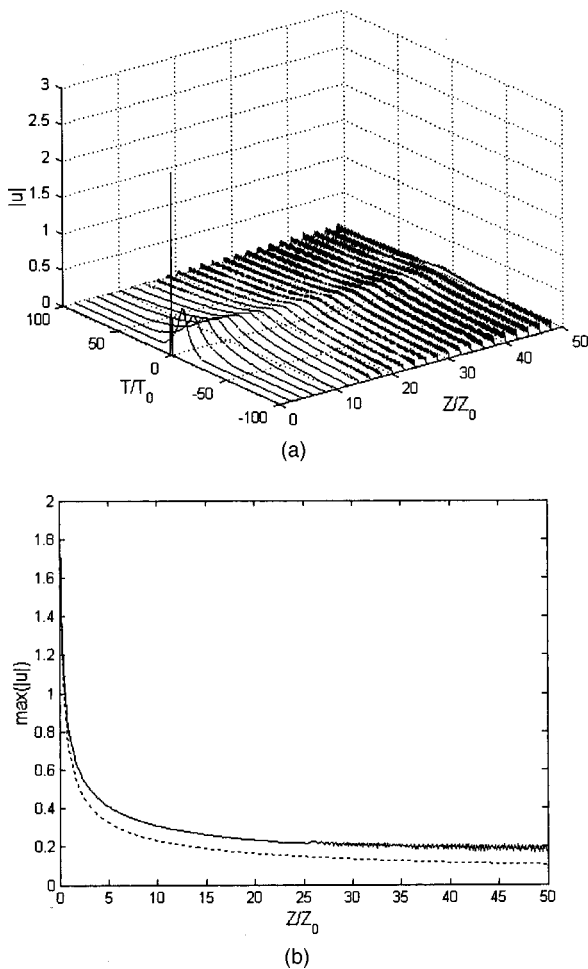


Fig. 7. Soliton spreading and decay of a soliton under the same configuration as in Fig. 6 but with initial width and chirp corresponding to a point $(\alpha, \alpha') = (0.2, 0.5)$ ($E_0 > 0$): (a) numerical integration of the NLS equation; (b) comparison of the direct simulation (solid curve) with the variational method (dashed curve).

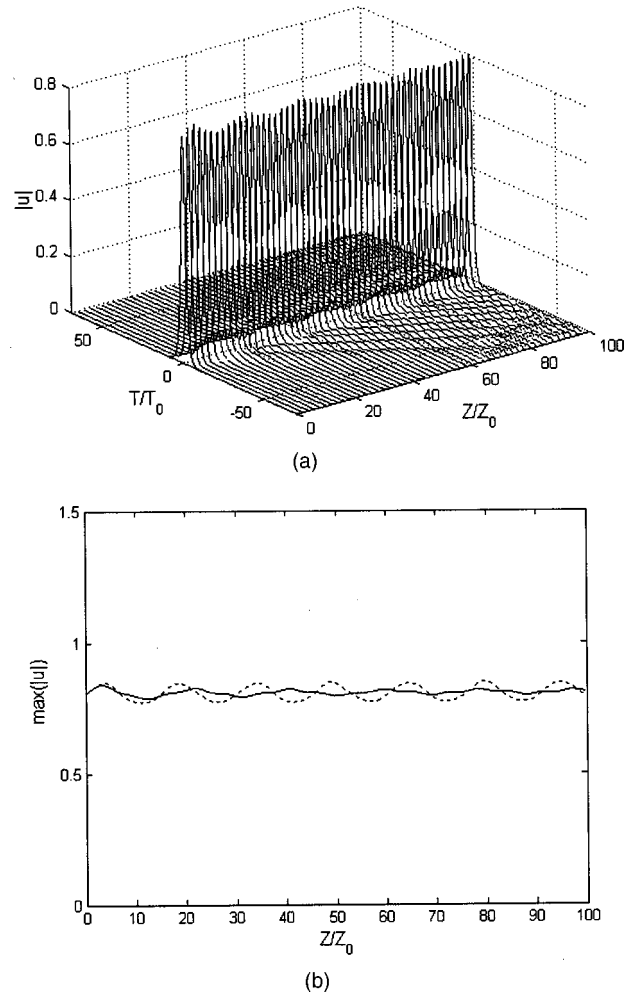


Fig. 8. Nonlinear shape oscillations of a soliton of $t_s = 8$ ps duration under amplification period $d = 100$ km. $N = 0.9$, corresponding to $\omega_0 \leq \Omega$. The initial width and chirp correspond to the point $(\alpha, \alpha') = (1.25, -0.04)$ in Fig. 4(a): (a) numerical integration of the NLS equation; (b) comparison of the direct simulation (solid curve) with the variational method (dashed curve).

3(d) by the fact that there exist some level curves surrounding both resonances, These level curves are not separated around each island and are not actual invariant curves. However, for small values of J (near the bottom of the potential well) and close to the center of each island there exist invariant (KAM) curves, which are successfully approximated by the level curves at these regions of the phase plane.

The case shown in Fig. 4 is similar to the previous one, but we take $N = 0.9$ so that $\omega_0 \leq \Omega$, which makes the (1, 1) and (2, 1) resonances impossible. In Fig. 4(b) all the resonances above the (4, 1) resonance have been merged to a stochastic sea, and only very close to the center of each island are there invariant curves confining the motion. Higher-order (in ϵ) resonances are also visible. In Fig. 4(d) are shown level curves surrounding two or even three islands of different resonances that are not actual invariant curves. Wherever there exist actual KAM curves, these curves are successfully approximated by the corresponding level curves.

The stochastic layer for the same parameters as in Figs. 1 and 2 is given in Figs. 5(a) and 5(b), respectively,

as obtained by iterating the separatrix map. One can see islands of stability corresponding to KAM curves embedded into a stochastic sea. Inside these islands there exist smaller islands along with their respective separatrices and the stochastic layers around them. This quasi-chaotic structure is usually referred to as intermittent motion and has very interesting and complicated statistical properties.

The previously mentioned results demonstrate the agreement between the analytical approach, as given by the approximate local invariants, and the numerical solution of the system of ordinary differential equations obtained by the variational method. In what follows, we compare results provided by use of the variational approach with direct numerical simulations of the NLS equation, for some characteristic cases. In Fig. 6(a) is shown the pulse propagation as obtained from the numerical integration of the NLS equation for the same t_s , N , and amplification distance d as in Fig. 3, with the initial width the chirp of the pulse chosen so that $(\alpha, \alpha') = (1.1, 0.1)$. Pulse amplitude as obtained by the variational method (dashed curve) and the direct simulation

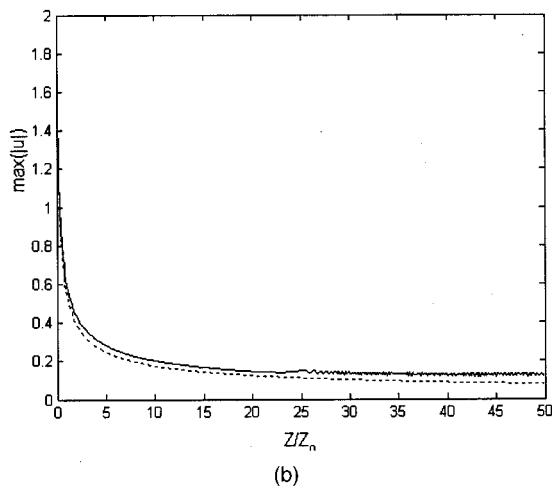
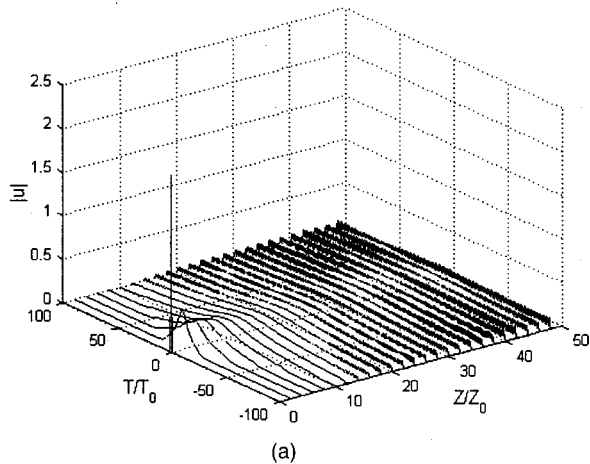


Fig. 9. Soliton spreading and decay of a soliton under the same configuration as in Fig. 8 but with initial width and chirp corresponding to a point $(\alpha, \alpha') = (0.2, 0.1)$ ($E_0 > 0$): (a) numerical integration of the NLS equation; (b) comparison of the direct simulation (solid curve) with the variational method (dashed curve).

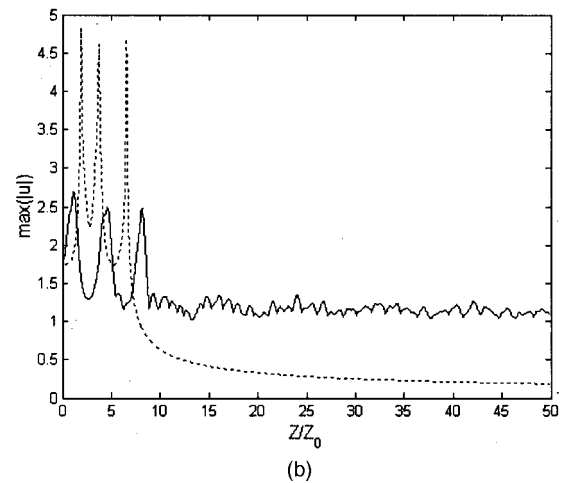
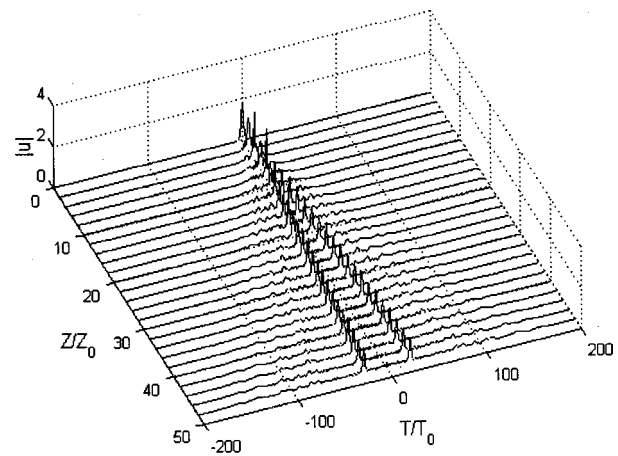


Fig. 10. Propagation and splitting of a soliton of $t_s = 13.6$ ps duration under amplification period $d = 40$ km. $N = 1.83$, corresponding to $\omega_0 = \Omega$. The initial width and chirp correspond to a point $(\alpha, \alpha') = (1, 0.5)$: (a) numerical integration of the NLS equation; (b) comparison of the direct simulation (solid curve) with the variational method (dashed curve).

(solid curve) is given in Fig. 6(b). The nonlinear shape oscillations of the pulse predicted by the variational approach for the specific set of parameters is confirmed by the direct simulation. However, the small difference between the results concerning the amplitude and the period of the oscillations is a consequence of the radiative losses ignored by the variational approximation. Figure 7 differs from the previous case in the initial width and chirp of the pulse, which are chosen so that $(\alpha, \alpha') = (0.2, 0.5)$. The effective particle initial energy E_0 is positive, and the pulse spreading predicted by the variational method is confirmed by the direct simulation as shown in Fig. 7(a). The pulse amplitude as obtained by the two methods is given in Fig. 7(b). The agreement between the results obtained by the variational method (dashed curve) and the direct numerical simulation (solid curve) is good. Moreover, it is evident from this figure that the variational method predicts a slightly more drastic pulse deterioration in accordance with similar observations.²³ In Figs. 8 and 9 we have the same t_s , N , and d as in Fig. 4, and the initial width and chirp of the

pulse are chosen so that $(\alpha, \alpha') = (1.25, -0.04)$ and $(\alpha, \alpha') = (0.2, 0.1)$, respectively. The same comments with the previous cases (Figs. 6 and 7) apply here as well. For a pulse of $t_s = 13.6$ ps and an amplification distance $d = 40$ km the dispersion distance is now $Z_0 = 46.11$ km, the normalized amplification distance is $Z_a = 0.867$, and the effective perturbation strength is quite large, $\epsilon = 0.5$, so the phase-plane analysis in these case clearly would lead to very chaotic dynamics. Choosing $N = 1.83$ so that $\omega_0 = \Omega$ and a pulse of initial width and chirp so that $(\alpha, \alpha') = (1, 0.5)$, we have a pulse propagating as in Fig. 10(a). The pulse splits into two secondary pulses of smaller amplitude after a few oscillation periods. This abrupt destruction of the pulse has also been demonstrated for the case where the pulse propagates under an inhomogeneity induced by a varying dispersion and for a quite similar perturbation strength ϵ .²³ In Fig. 10(b) we compare results obtained by direct simulation and the variational method, respectively. The qualitative picture as described by the motion of the effective particle is that of an intermittent type: The initial energy of the particle E_0 is negative, but the quite strong perturbation results in escaping from the potential well after the particle spends a few periods near a resonant center. It is quite remarkable that, although the variational approximation cannot capture such a drastic change in the pulse shape, it still gives an accurate estimation of the number of oscillations that a pulse undergoes before it splits into the secondary pulses and the propagation distance at which this abrupt splitting takes place as well.

7. CONCLUSIONS

In this paper the chirped-pulse propagation under periodic amplification was considered from the point of view of communication applications where standard approaches (such as the guiding-center theory) usually fail. The results obtained by the variational method were compared with those from the direct integration of the NLS equation for some characteristic values of the pulse parameters at the launching point. The comparison has shown a satisfactory agreement. The presence of nonlinear shape oscillations suggested by the variational method was actually confirmed by the numerical integration of the NLS equation. Furthermore, the spreading/decay of the pulse for a certain range of launching-pulse characteristics, as predicted by the variational method, was also confirmed for small values of perturbation strength ϵ . For larger values of perturbation the pulse was shown to split into two pulses after propagating through a few amplification periods. Although the variational method cannot describe such a drastic pulse-shape change, it still provides an estimation of the distance that the pulse propagates as well as the number of oscillations the pulse undergoes before its shape changes drastically.

The paper was focused on the construction, by the canonical perturbation method, of local approximate invariants as well as the application of Melnikov's method for the investigation of the structure and the width of the stochastic layer between the two distinct modes of behavior of the propagating pulse, namely, the breathing and

spreading/decaying. The aforementioned invariants contain all the essential features of the phase space of the system and reveal the intrinsically inhomogeneous structure of the chaotic regions. The existence of KAM surfaces even for moderate values of the perturbation strength points toward the possibility of robust pulse propagation even under "harsh" conditions imposed by technological constraints. The role of the parameters involved in what is usually called "perturbation strength" was fully clarified and investigated by realistic examples of applications. The approximate invariants can provide useful guidelines for choosing the appropriate launching-pulse parameters (width and chirp), in order to provide stable (oscillatory) propagation, for each specific configuration of the transmission link (amplifier spacing and pulse-launching energy). As far as the calculation of the width of the stochastic layer near the separatrix is concerned, we confined ourselves to small values of the perturbation strength (~ 0.005 or less), since the method is absolutely reliable for such values. The latter ease's the applicability of the separatrix map as a tool of obtaining the width of the stochastic layer. The use of the separatrix mapping in order to estimate escaping times for various initial (launching) conditions, and consequently the number of amplification stages that a pulse can propagate before decay or splitting, is another interesting feature that is the subject of a future study. Realistic examples are given for pulse width in the range of 4 to 14 ps and for amplification periods of 40–100 km.

ACKNOWLEDGMENTS

The authors are indebted to the late Chronis Polymilis for useful discussions. This research has been supported in part by the Archimedes Grant of the Institute of Communications and Computer Systems/National Technical University of Athens and in part by the General Secretariat of Research and Development under contract PENED-95/644.

REFERENCES

1. A. Hasegawa and Y. Kodama, *Solitons in Optical Communications* (Clarendon, Oxford, 1995).
2. M. Nakazawa, Y. Kimura, and K. Suzuki, "Soliton amplification and transmission with Er^{3+} -doped fiber repeater pumped by GaInAsP laser diode," *Electron. Lett.* **25**, 199–200 (1989).
3. R. G. Bauer and L. A. Melnikov, "Multi-soliton fission and quasi-periodicity in a fiber with a periodically modulated core diameter," *Opt. Commun.* **115**, 190–198 (1995).
4. I. Gabitov, E. G. Shapiro, and S. K. Turitsyn, "Asymptotic breathing pulse in optical transmission systems with dispersion compensation," *Phys. Rev. E* **55**, 3624–3633 (1997).
5. S. K. Turitsyn, I. Gabitov, E. W. Laedke, V. K. Mezentsev, S. L. Musher, E. G. Shapiro, T. Schäfer, and K. H. Spatschek, "Variational approach to optical pulse propagation in dispersion compensated transmission systems," *Opt. Commun.* **151**, 117–135 (1998).
6. H. Sugahara, K. Hiroki, I. Takashi, A. Maruta, and Y. Kodama, "Optimal dispersion management for a wavelength division multiplexed optical soliton transmission system," *J. Lightwave Technol.* **17**, 1547–1559 (1999).
7. B. A. Malomed, D. F. Parker, and N. F. Smyth, "Resonant shape oscillations and decay of a soliton in a periodically in-

- homogeneous nonlinear optical fiber," *Phys. Rev. E* **48**, 1418–1425 (1993).
8. B. A. Malomed, "Pulse propagation in a nonlinear optical fiber with periodically modulated dispersion: variational approach," *Opt. Commun.* **136**, 313–319 (1997).
 9. T. I. Lakoba, J. Yang, D. J. Kaup, and B. A. Malomed, "Conditions for stationary propagations in the strong dispersion management limit," *Opt. Commun.* **149**, 366–375 (1998).
 10. J. N. Kutz, P. Holmes, S. G. Evangelides, and J. P. Gordon, "Hamiltonian dynamics of dispersion-managed breathers," *J. Opt. Soc. Am. B* **15**, 87–96 (1998).
 11. P. Holmes and J. N. Kutz, "Dynamics and bifurcations of a planar map modeling dispersion managed breathers," *SIAM J. Appl. Math.* **59**, 1288–1302 (1999).
 12. I. Gabitov and S. K. Turitsyn, "Averaged pulse dynamics in a cascaded transmission system with passive dispersion compensation," *Opt. Lett.* **21**, 327–329 (1996).
 13. J. P. Gordon, "Dispersive perturbations of the nonlinear Schrödinger equation," *J. Opt. Soc. Am. B* **9**, 91–97 (1992).
 14. N. J. Smith and N. J. Doran, "Picosecond soliton transmission using concatenated nonlinear optical loop-mirror intensity filters," *J. Opt. Soc. Am. B* **12**, 1117–1125 (1995).
 15. R.-J. Essiambre and G. P. Agrawal, "Soliton communication beyond the average-soliton regime," *J. Opt. Soc. Am. B* **12**, 2420–2425 (1995).
 16. W. Forysiak, N. J. Doran, F. M. Knox, and K. J. Blow, "Average soliton dynamics in strongly perturbed systems," *Opt. Commun.* **117**, 65–70 (1995).
 17. Z. M. Liao, C. J. McKinstrie, and G. P. Agrawal, "Importance of prechirping in constant-dispersion fiber links with a large amplifier spacing," *J. Opt. Soc. Am. B* **17**, 514–518 (2000).
 18. F. Kh. Abdullaev and J. G. Caputo, "Validation of the variational approach for chirped pulses in fibers with periodic dispersion," *Phys. Rev. E* **58**, 6637–6648 (1998).
 19. F. Kh. Abdullaev, A. A. Abdumalikov, and B. B. Baizakov, "Stochastic instability of chirped optical solitons in media with periodic amplification," *Quantum Electron.* **27**, 171–175 (1997).
 20. D. Anderson, "Variational approach to nonlinear pulse propagation in optical fibers," *Phys. Rev. A* **27**, 3135–3145 (1983).
 21. D. Anderson, M. Lisak, and T. Reichel, "Asymptotic propagation properties of pulses in a soliton-based optical-fiber communication system," *J. Opt. Soc. Am. B* **5**, 207–210 (1988).
 22. E. A. Kuznetsov, A. V. Mikhailov, and I. A. Shimokhin, "Nonlinear interaction of solitons and radiation," *Physica D* **87**, 201–215 (1995).
 23. R. Grimshaw, J. He, and B. A. Malomed, "Decay of a fundamental soliton in a periodically modulated nonlinear waveguide," *Phys. Scr.* **53**, 385–393 (1996).
 24. B. A. Malomed, "Resonant transmission of a chirped soliton in a long optical fiber with periodic amplification," *J. Opt. Soc. Am. B* **13**, 677–686 (1996).
 25. H. Gylden, "Die Bahnbewegung in einem Systeme von zwei Körpern in dem Falle dass die Massen Veränderungen unterworfen sind," *Astron. Nachr.* **109**, 1–6 (1884).
 26. A. J. Lichtenberg and M. A. Leiberman, *Regular and Stochastic Motion* (Springer-Verlag, New York, 1983).
 27. H. Goldstein, *Classical Mechanics* (Addison-Wesley, Reading, Mass., 1980).
 28. B. V. Chirikov, "A universal instability of many-dimensional oscillator systems," *Phys. Rep.* **52**, 263–379 (1979).
 29. J. Guckenheimer and P. Holmes, *Nonlinear Oscillations, Dynamical Systems, and Bifurcations of Vector Fields* (Springer-Verlag, New York, 1983).
 30. F. Diacu and D. Şelaru, "Chaos in the Gylden problem," *J. Math. Phys.* **39**, 6537–6546 (1998).
 31. G. M. Zaslavsky, "The width of exponentially narrow stochastic layers," *Chaos* **4**, 589–591 (1994).
 32. J. B. Taylor and E. W. Laing, "Invariant for a particle interacting with an electrostatic wave in a magnetic field," *Phys. Rev. Lett.* **35**, 1306–1307 (1975).